Vibrational line broadening in the solid system N2-Kr

Lotz, Heidi T.; Michels, Jan P. J.; Schouten, Jan A.

Published in:
The Journal of Chemical Physics

DOI:
10.1063/1.1477189

Vibrational line broadening in the solid system N_2–Kr: A molecular dynamics study

Heidi T. Lotz, Jan P. J. Michels, and Jan A. Schouten

Citation: J. Chem. Phys. **117**, 7245 (2002); doi: 10.1063/1.1477189
View online: https://doi.org/10.1063/1.1477189
View Table of Contents: http://aip.scitation.org/toc/jcp/117/15
Published by the American Institute of Physics

Vibrational line broadening in the solid system N_2-Kr: A molecular dynamics study

Heidi T. Lotz,[a] Jan P. J. Michels,[b] and Jan A. Schouten[c]
Van der Waals-Zeeman Institute, University of Amsterdam, Valckenierstraat 65, 1018 XE, Amsterdam, The Netherlands

(Received 27 August 2001; accepted 19 March 2002)

The vibrational band shapes and the related parameters of N_2 in Kr have been calculated by molecular dynamics simulations as a function of the nitrogen concentration. Most of the simulations have been applied to the solid hcp phase at 5 GPa and 296 K. The calculated spectra have been obtained by full analysis of the relaxation function. Due to the limited size of the system, the particles remain near the same lattice point throughout a simulation run (no N_2-Kr exchange). Upon dilution, the vibrational frequency of nitrogen in krypton shows a red shift. The full width at half maximum is extremely composition dependent, with a maximum value of 3.5 cm^{-1} at equal mole fractions. In addition, for the 50 and 75 mol % systems, a few special configurations with ordered distributions have been simulated. On the basis of these results together with earlier experimental data it is suggested that, in the real solid system, the nitrogen and krypton particles exchange places rapidly so that in time, each N_2 molecule vibrates with all possible frequencies. To make an estimation of the exchange rate, several simulations have been performed during which the particles exchange randomly at various rates. The calculated widths depend strongly on the exchange rate. By comparison of the calculated and the experimental width of the spectra, an estimation of the exchange rate in the real system is made. © *2002 American Institute of Physics.*
[DOI: 10.1063/1.1477189]

INTRODUCTION

In the past decade many attempts, either analytical[1–13] or by computer simulations[14–22] have been made to calculate the line shift and linewidth of the Raman spectra in simple binary fluids at ambient and elevated pressures. In particular the Raman *Q* branch of nitrogen has been the subject of extensive studies. In earlier papers it was found that the linewidth in the fast and slow modulation regime can be calculated from molecular dynamics simulations, using the Kubo theory.[23] Depending on the type of modulation, the width of the modulated signal $I(\omega)$ is more or less reduced compared to the momentary frequency distribution, due to motional narrowing. The theoretical model of Knapp and Fischer[1,5] describes the change of the shape of the spectrum $I(\omega)$ as a function of the mole fraction x for binary liquids. Within this model, the linewidth can be calculated from the total line shift between the neat liquid and infinite dilution.

Bondarev and Mardaeva[24] were the first to show experimentally that in liquid binary mixtures the composition dependence of the linewidth shows a maximum at about equal mole fractions while the line center is linearly shifted upon dilution. In a previous paper,[25] we reported an experimental study on the composition dependence of the spectral line shape of nitrogen in the mixed solid N_2-Kr. It was shown in that study that, also in the solid phase, the linewidth is strongly composition dependent, with maximum values five times as high as in the neat system. It was suggested that the broadening is due to an increase of the correlation time rather than an increase in the amplitude of modulation. In this paper, in order to verify this assumption and to obtain more information about the underlying mechanisms, we report molecular dynamics simulations of nitrogen in krypton for several concentrations at 296 K in the pressure range 0.7–9.75 GPa.

METHODS

A full description of the procedure applied for calculation of the vibrational frequency from molecular dynamical calculations can be found in previous papers.[26–29] For convenience of the reader, the method is given briefly below.

The nitrogen molecule has been modeled by a site-site potential with a fixed interatomic distance of 1.094 Å. For the interactions between the sites of distinct nitrogen molecules, the van der Waals profile of the Etters[30] potential was used. By omitting the quadrupolar term, the model was reduced to a site-site potential

$$\frac{\Phi(r)}{\kappa_B} = A_1 e^{-\alpha_2 r} - B_1 r^{-6}, \quad r < R_0,$$

$$\frac{\Phi(r)}{\kappa_B} = \sum_{i=0}^{4} C_i (r - R_0)^n - B_1 r^{-6}, \quad R_0 < r \leq R_1,$$

$$\frac{\Phi(r)}{\kappa_B} = A_2 e^{-\alpha_1 r} - B_1^{-6}, \quad r > R_1, \tag{1}$$

with

[a]Electronic mail: h.lotz@nki.nl
[b]Electronic mail: jmichels@science.uva.nl
[c]Electronic mail: schouten@science.uva.nl

$A_1 = 9.261205 \times 10^7$ K, $C_3 = -2766.5419$ K Å^{-3},

$A_2 = 1.47248 \times 10^7$ K, $C_4 = 1574.2809$ K Å^{-4},

$B_1 = 1.79 \times 10^5$ K Å^6, $R_0 = 3.01006875$ Å,

$C_0 = 415.73107$ K, $R_1 = 3.4494569$ Å,

$C_1 = -1446.74414$ K Å^{-1}, $\alpha_1 = 4.037$ Å^{-1},

$C_2 = 2480.73711$ K Å^{-2}, $\alpha_2 = 3.48$ Å^{-1}.

For the krypton-krypton and the nitrogen-krypton interactions exponential-6 potentials have been taken:

$$\Phi(r) = \frac{6\varepsilon}{\alpha - 6}\left[e^{\alpha(1-(r/r_m))} - \alpha\left(\frac{r_m}{r}\right)^6 \right], \tag{2}$$

with r the distance between a N site and a Kr atom and with parameter values, α the stiffness of the repulsive part of the potential, ε the well depth, and r_m the diameter at the minimum:

$\alpha = 12.3$, $\varepsilon/\kappa_B = 158.3$ K,

$r_m = 4.056$ Å for the Kr-Kr potential Ref. 31,

$\alpha = 13.38$, $\varepsilon/\kappa_B = 78.97$ K,

$r_m = 3.893$ Å for the N_{atom}-Kr potential

($\alpha = 14.55$, $\varepsilon/\kappa_B = 39.4$ K,

$r_m = 3.73$ Å, N_{atom}-N_{atom}).

Note that the last quoted parameters are merely used to calculate the N_{atom}-Kr parameters with the use of the Lorentz-Berthelot rule. Four mechanisms that contribute to the vibrational frequency have been considered:

(i) The external force, exerted by the surrounding molecules and acting along the molecular axis (first-order contribution).

(ii) The derivative of the external force to the bond length (second-order contribution).

(iii) The vibration-rotation coupling (VR).

(iv) The dispersion correction (DC) due to the change in polarizability at excitation.

From this, the time average of the total change in the vibrational frequency ω_{vib}, the amplitude of modulation Δ, the autocorrelation function of the frequency $\Omega(t)$, the correlation time τ_c, and the relaxation function $\varphi(t)$ have been derived with

$$\Delta = \sqrt{\langle \omega_{vib}^2 \rangle - \langle \omega_{vib} \rangle^2}, \tag{3}$$

$$\Omega(t) = \frac{\langle \omega_{vib}(0)\omega_{vib}(t) \rangle - \langle \omega_{vib}(0) \rangle^2}{\Delta^2}, \tag{4}$$

$$\tau_c = \lim_{t\to\infty} \int_0^t \Omega(s)\,ds, \tag{5}$$

$$\varphi(t) = \left\langle \exp\left(i \int_0^t \omega(t')\,dt' \right) \right\rangle. \tag{6}$$

Since the total change in the vibrational frequency ω_{vib}, due to surrounding molecules, consists of the four mentioned contributions, the total correlation function contains self-correlations and cross terms. Hence, the correlation time consists of a sum of terms for each of the effects.[28]

The change in potential energy at excitation (DC) was calculated directly from the difference in frequency between the experimental and the simulated data, as will be described below. To derive the parameters for the dispersion correction for nitrogen in krypton at various concentrations, the DCs for solid nitrogen ($x = 1$) and for the infinite dilution of nitrogen in krypton ($x = 0$) have been determined.

The chosen DC potential[28] that accounts for the pressure dependence of the energy gap between the experimental and the calculated frequency for fluid nitrogen without DC has the form

$$\frac{\Delta\Phi}{\kappa_B T} = \left(\frac{a}{r}\right)^{12} - \left(\frac{b}{r}\right)^6. \tag{7}$$

The parameters for fluid N_2 have been determined previously.[26] In order to derive the parameters for solid nitrogen ($a = 2.760$ Å and $b = 2.738$ Å) three simulation runs have been performed, simulating a box with 384 particles in hcp configuration at 296 K, at pressures just above the fluid-solid transition. From the simulation runs the vibrational frequency without DC, as a function of pressure, was achieved. The experimental data are taken from Ref. 32 using the expression

$$\nu = 2323.65 + 5.264p - 0.2783p^2. \tag{8}$$

To determine the parameters for the DC for nitrogen in krypton, several simulation runs were carried out for one nitrogen molecule in a box with 255 krypton atoms (infinite dilution of nitrogen in krypton). Since the vibrational frequency is linearly dependent on x, the experimental data was linearly extrapolated to $x = 0$. The parameters for the DC term then were obtained by fitting the calculated values with the experimental data. Doing so, no suitable parameters could be realized using formula (8). Instead, a DC term of the form

$$\frac{\Delta\Phi}{\kappa_B T} = -\left(\frac{a}{r}\right)^8 - \left(\frac{b}{r}\right)^6, \tag{9}$$

with $a = 3.024$ Å and $b = 2.862$ Å (solid fcc phase) and $a = 3.146$ Å and $b = 2.587$ Å (fluid phase), turned out to be satisfactory.

The two potentials might seem quite different but, since both terms have the same sign: e.g., a decrease in a and the corresponding increase in b results in a fit with only a slightly different standard deviation. The two reasons for the difference in the DC of a solid and a fluid are the following. First, for a given distance between two atoms of two different molecules, the interaction depends on the relative orientations of the molecules. These are more or less random in a fluid but there are preferred orientations in the solid.[19] Second, the configuration of the set of molecules plays a role. Let us consider, e.g., the effect of the three-particle interaction between two particles separated by a distance r. In the fluid, the third particle can be almost anywhere but in the solid, the positions of the third particle are close to the lattice points. Thus, the average effect is different. Both effects are important for, e.g., structure calculations,[33] but as has been

shown previously,[27] the details of the potential only slightly influence the first and second-order contributions to the Raman frequency. However, in chemical terms, the DC is the difference in solvation energy between excited and nonexcited molecules. Compared to the energy of vibration, the solvation energy is large in both cases and small changes in both values may result in large changes in the difference.

In the following, a few remarks concerning the chosen potential are made. For N_2 in Ar (Ref. 34) and N_2 in Ne (Ref. 21) a suitable DC potential could be established using the general form of Eq. (7). For N_2 in Xe (Ref. 20) this form did not suit and instead only an r^{-6} term was used. The need of the repulsive part (r^{-12}) could be related to the size of the atoms. While for small atoms (Ar and Ne) this repulsive part is necessary, for large atoms (Xe) the term is not needed as the particles probably do not approach as close as in the case of small atoms.

For N_2 in Kr (krypton is slightly larger argon) no correct adjustment could be realized using only the r^{-6} term. Adding a repulsive part did not cause any improvement. Instead, the r^{-8} term, which is the next term in the progression of the dispersion expansion, was used. Finally, it must be mentioned that, for nitrogen, no correct adjustment could be realized using an r^{-8} term.

RESULTS

The molecular dynamics (MD) simulations of the solid mixtures of krypton and nitrogen have been carried out on model systems in a box provided with periodic boundaries, consisting of 384 and 256 particles for the hcp and fcc configurations, respectively. The calculations have been performed in the pressure range 0.7–9.75 GPa at 296 K. The systems consisted of N_2 mole fractions $x=0$, 0.25, 0.50, 0.75, and 1. For nitrogen infinitely diluted in krypton ($x=0$) the system consisted of one single N_2 molecule in a Kr bath. All registrations were made with equidistant time steps of 0.01 ps throughout a simulation time of 1000–3000 ps. Since krypton solidifies in the fcc structure, this configuration is used for $x=0$ (1 N_2 particle in 255 Kr particles). All other model systems have been simulated using the hcp lattice. It must be mentioned that simulation results for pure nitrogen and also previous results on nitrogen in argon (not published) showed no significant difference in the frequency for the hcp and fcc lattices. As the diameters of Kr and N_2 correspond even better than those of Ar and N_2 we can assume that also for nitrogen in krypton the frequencies in the hcp and fcc structures will be similar. It should be noticed that, due to the limited size of the system, the chance of spontaneous swaps to take place in the mixed solid phase is very small. Hence, although no constraints are imposed, the particles do not spontaneously exchange places in the solid. For the mixed solids, a few random configurations have been simulated for each composition. In addition, for the 50 and 75 mol % systems, a few special configurations, as described below, have been investigated.

For the 50 mol % mixture, the following was found:

(A) Starting with a box provided with periodic boundaries and composed of eight layers of N_2 particles, every other layer is replaced by a layer with Kr particles. In this way the system consists of equal mole fractions N_2 and Kr and the surroundings of all particles are equal. Considering only nearest neighbors, each N_2 particle is surrounded by six N_2 and by six Kr particles.

(B) Again the system consists of equal mole fractions N_2 and Kr but now two different surroundings are created. Starting with a box composed of N_2 particles, every other molecule is replaced by a Kr particle in such a way that half of the nitrogen molecules have four N_2 and eight Kr particles as neighbors and the other half is surrounded by six N_2 and six Kr particles. Hence, we have two ''types'' of molecules.

For the 75 mol %, mixture the following was found:

(C) The Kr particles are placed on top of the N_2 particles in the following order: six layers N_2 and two layers Kr. Taking only nearest neighbors into account, this configuration results in two ''types'' of molecules: molecules that are completely surrounded by N_2 and those that are surrounded by nine N_2 and three Kr particles.

(D) A Kr cluster with spherical shape (25% of the particles), surrounded by N_2 particles. With this configuration, many distinct molecules are simulated with numbers of N_2 neighbors ranging from 1 up to 12.

(E) A N_2 cluster (75% of the particles), surrounded by Kr particles, again giving many ''types'' of N_2 molecules.

For all other simulations, random configurations were generated.

The calculated spectra are obtained by Fourier transformation of the relaxation function

$$I(\omega)=\frac{1}{2\pi}\int_{-\infty}^{\infty} e^{-i\omega t}\varphi(t)dt. \tag{10}$$

Figure 1 shows the absolute value of three typical relaxation functions, plotted on a linear [Fig. 1(a)] and on a logarithmic scale [Fig. 1(b)] for mole fractions $x=1$ and $x=0.75$, system C, and for a random configuration with $x=0.75$. The corresponding spectra are presented in Fig. 2. The behavior of the relaxation functions for all random configurations is comparable to the one plotted in the figure (dashed line) except for the fact that, for the mixtures with equal mole fractions, the decay occurs somewhat faster. The relaxation functions for $x=0$ and for system A ($x=0.50$) are comparable with that of neat nitrogen but with slightly faster decay. Clearly, the fastest decay occurs for the mixtures with random configurations.

In earlier studies[21] it was shown that, by straightforward transformation of the relaxation function, the obtained profile is seriously smudged by noise which is caused by considerable scatter in the relaxation function at large values of t. Kubo has shown that, for any stochastic process with $\omega(t)=\omega_0+\omega_1(t)$, the absolute value of the relaxation function decays exponentially for $\tau \gg \tau_c$ while the bulk information about the profile is stored in the initial part of $\varphi(t)$. Therefore, in order to improve statistics, for the ''pure'' systems the relaxation function has been fitted with an exponential function in the range $t_m<t<t_n$. The values of the relaxation function are replaced by those of the exponential fit for $t>t_n$. It has been verified that the exponential decay is set in at $t<t_m$ and also, that the results in the width are not sensi-

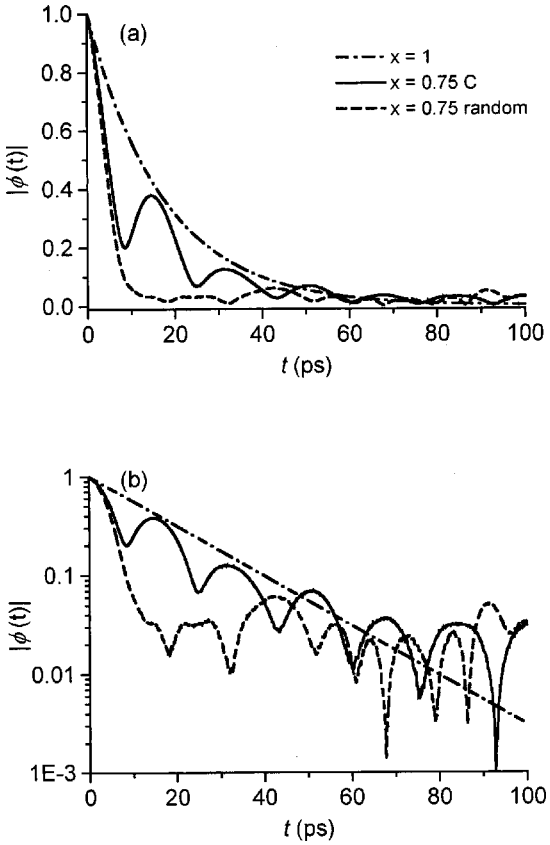

FIG. 1. Absolute value of typical relaxation functions for several configurations in the hcp lattice at 5.0 GPa and 296 K, plotted on a linear scale (a) and on a logarithmic scale (b). All functions have been replaced by an exponential fit up from 120 ps. Dash-dotted line: $x=1$; solid line: $x=0.75$, system C; dashed line: $x=0.75$, random configuration.

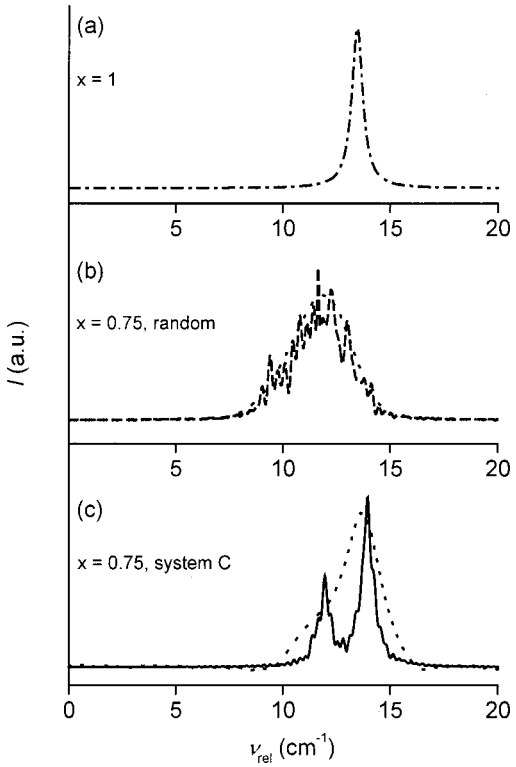

FIG. 2. MD spectra concerning hcp configurations at 5.0 GPa, obtained by Fourier transformation of the relaxation functions that are plotted in Fig. 1. All line types and symbols correspond to those in Fig. 1. (a) $x=1$; (b) $x=0.75$, random configuration; (c) $x=0.75$; system C.

tive to the choice of the range. A full description of the applied procedure is given in Ref. 29.

For all mixed systems, except system A, the situation is complex. Since not all molecules have the same surroundings and the configuration is static, apart from vibrations around the lattice positions, different frequencies ω_0 for the distinct molecule ''types'' exist. Consequently, some of the contributions to the frequency correlation function show a limiting value not equal to zero. Hence, the correlation time defined in Eq. (5) is infinite. Therefore τ_c is not an appropriate parameter for these systems. The relaxation functions for these mixtures consist of a superposition of curves [Figs. 1(a) and 1(b)]. These functions have been treated in the following way. After thorough investigation it was found that, by fitting $\varphi(t)$ in the range $0 \leqslant t < t_n$ with an exponential function and replacing the tail ($t > t_n = 120$ ps) by the fit, the line shape of the obtained spectra is not sensitive to the choice of t_n for values of $t_n > 100$ ps but the scatter is reduced considerably. The spectra derived in this way show multiple peaks, as can be seen in Fig. 2(b) (dashed line). It must be mentioned that these peaks are reproducible and are caused by the discrete distributions since repeated simulations with identical configurations but different starting velocity distributions result in similar spectra. Note that the sinelike curved scatter in the wings in Fig. 2(c) is caused by a small discontinuity in the slope of the relaxation function at the point were the exponential fit starts.

In contrast with the experimental spectra, the calculated spectra show several peaks and are therefore difficult to compare with the experimental spectra. For that reason, all spectra stemming from the mixtures, except for system A, have additionally been smoothened. The resulting spectra, also shown in Fig. 2 (dotted lines), consist of a single peak and can be used for comparison with the experimental spectra.

The numerical results are given in Table I. In the third column the full width at half maximum (FWHM) is given. Column 4 shows the peak positions of the calculated spectra. Next, the frequency change with respect to the frequency of an isolated, nonrotating molecule[35] ($\nu_0 = 2329.91\ \mathrm{cm}^{-1}$) is given. In column 6 the mean frequency of the momentary distribution function is given. The amplitude of modulation, defined in Eq. (3) and given in wave numbers $\Delta/2\pi c$, is denoted in column 7.

First, let us compare the MD results for the random configurations with those of the pure systems. A selection of the spectra is depicted in Fig. 3. All spectra have been fitted with a Lorentzian curve (solid line). The spectra for $x=0.25$, 0.50, and 0.75 have also been fitted with a Gaussian curve (dashed line). For the neat N_2 system and for $x=0$ the relaxation function decays exponentially already for very small t and very slowly. As a result, the calculated line shape [Fig. 3(a)] is Lorentzian and the FWHM is small. Hence, these systems are in the fast modulation regime. For the mixtures, the relaxation function does not decay exponentially for small t.

TABLE I. Analysis results of MD simulations at 5.0 GPa. For an explanation of the configurations, see the text.

x	Config.	FWHM (cm^{-1})	Line shift (cm^{-1})	Rel. line shift (cm^{-1})	ν_{mean} of $P(\nu)$ (cm^{-1})	$\Delta/2\pi c$ (cm^{-1})
0 (fcc)		0.62	2338.12	8.212	8.212	6.065
0.25	random	2.78	2338.56	8.65	8.869	6.567
0.25	random	2.94	2338.62	8.71	8.875	6573
0.25	random	2.73	2338.41	8.5	8.604	6.517
0.25	random	2.89	2338.72	8.81	8.943	6.579
0.25	random	2.33	2338.48	8.57	8.676	6.505
0.50	random	2.71	2339.78	9.87	9.851	6.832
0.50	random	3.65	2339.94	10.03	10.02	6.886
0.50	random	3.21	2339.80	9.89	9.963	6.845
0.50	random	2.68	2339.67	9.76	9.733	6.792
0.50	A	0.63	2340.11	10.2	10.2	6.809
0.50	B	1.37	2339.22	9.31	9.314	6.720
0.75	C	1.9	2343.32	13.41	13.27	7.274
0.75	D	1.9	2341.11	13.2	12.92	7.255
0.75	E	2.03	2343.08	13.17	12.94	7.290
0.75	random	3.13	2343.69	11.78	11.7	7.121
0.75	random	3.14	2341.54	11.63	11.58	7.110
0.75	random	3.19	2341.48	11.57	11.55	7.120
0.75	random	3.32	2341.66	11.75	11.67	7.138
0.75	random	2.73	2341.55	11.64	11.57	7.095
1		0.61	2343.37	13.46	13.46	7.250

Therefore the calculated line shape deviates from a Lorentzian curve and has a large Gaussian component, as can be seen in Figs. 3(b) and 3(c). Since the decay occurs much faster compared to the neat systems, the widths of the spectra are much larger. Moreover, for $x=0.25$ and $x=0.75$, the spectra are asymmetrical, as can be seen in Fig. 3(c). For $x=0.25$ the points of the wing at the high-frequency side of the spectrum have a higher intensity than the Gaussian curve. The same effect can be observed for $x=0.75$ but now the wing is situated at the low-frequency side of the spectrum.

The composition dependence of the amplitude of modulation is depicted in Fig. 4. It is clear that, for the random configurations, the amplitude of modulation increases monotonically with x. For the infinite dilution ($x=0$) and for pure

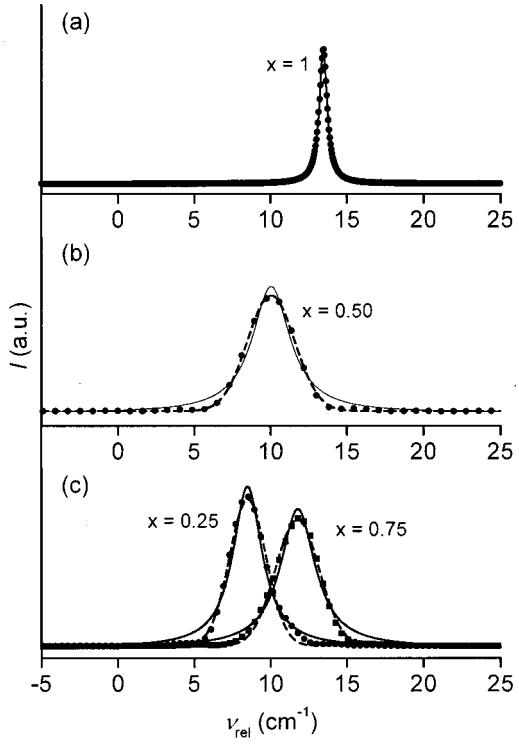

FIG. 3. MD spectra concerning random hcp configurations at 5.0 GPa, obtained by Fourier transformation of the relaxation functions. Symbols: simulation data; solid lines: Lorentzian fits; dashed lines: Gaussian fits.

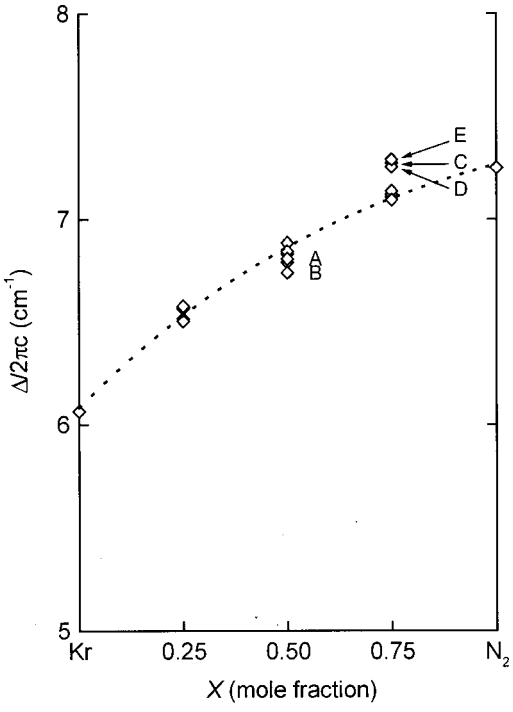

FIG. 4. Amplitude of modulation as function of the N_2 mole fraction at 5.0 GPa. Special configurations are indicated with capitals A–E and are explained in the text. The dashed line is a guide to the eye through the data with random configurations.

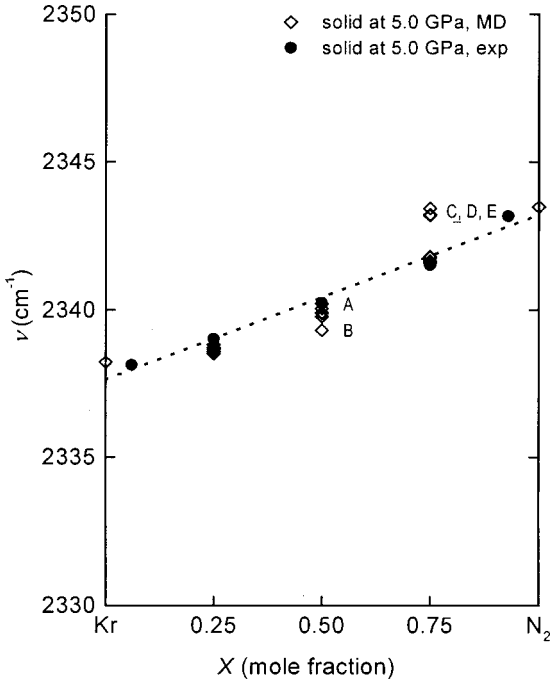

FIG. 5. Vibrational frequency of nitrogen diluted in Kr (Ref. 25) vs the mole fraction at 5.0 GPa (solid) and 0.7 GPa (fluid). Open symbols: simulation data; solid symbols: experimental data. Squares: fluid phase; circles: homogeneous hcp phase. The dotted line represents a linear fit through the experimental data points.

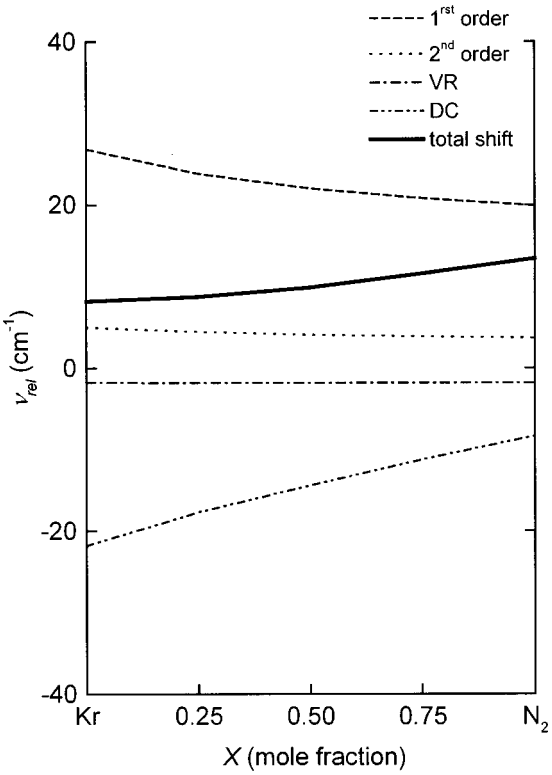

FIG. 6. Individual contributions to the calculated frequency of nitrogen diluted in Kr relative to the isolated, nonrotating molecule ($\nu_0 = 2329.91\ \mathrm{cm}^{-1}$) together with the total relative shift.

N_2 at 5.0 GPa, $\Delta/2\pi c = 6.05$ and 7.25, respectively. The values for the intermediate concentrations are situated on a curved line in between both extremes.

The vibrational frequency as function of the concentration is shown in Fig. 5. For comparison, the experimental data at 5.0 GPa, taken from Ref. 25, are also plotted in the figure (solid circles) ($x = 0.06$: fcc; $x = 0.25$, 0.50, 0.75, and 0.93: hcp). All experimental points except those for pure N_2 have been obtained by linear interpolation. The experimental values for pure β-N_2 have been obtained by linear extrapolation, since pure nitrogen is in the δ phase at this pressure. As in the fluid phase, the vibrational frequency in the solid increases monotonically with x. Moreover, while the peak positions for the random configurations are in agreement with the experimental data, those for the ordered configurations deviate from the experimental values. In Fig. 6 the four individual contributions (first and second order, VR, and DC) to the relative frequency shift as well as the total relative shift are shown. The figure shows that the DC contribution to the frequency is substantial, especially for high krypton concentrations. Moreover, the composition dependence is mainly caused by the DC and to a lesser degree by the first order effect, while the second order effect and, of course the VR, are not significantly sensitive to the concentration.

The FWHM of the calculated spectra as well as the experimental values are plotted against the mole fraction in Fig. 7. For molecular dynamics simulations as well as for real systems, a maximum in the width occurs at about equal mole fractions. In the fluid phase (0.7 GPa, squares), the calculated linewidths agree well with the experimental data. However, comparing the values in the solid phase (5.0 GPa, circles) with the experimental data, it is clear that there is qualitative agreement but the widths of the calculated spectra are considerably higher.

Regarding the layered and clustered configurations, the situation is quite different. Since system A has been set up in such a way that each particle has the same number of N_2 and Kr particles as nearest neighbors, one expects a single frequency distribution with a peak position comparable to those of the random configurations with $x = 0.50$, which is indeed the case. Yet because of this single distribution, the width is much smaller than those of the random configurations at $x = 0.50$ and in fact comparable with $x = 0$ and $x = 1$. Not only the linewidth but also the relaxation function and therefore the Lorentzian and symmetrical line shape are comparable with that of the latter two systems. Hence, this system is in fast modulation. Also interesting are the mixtures in which two or more different surroundings are created. Regarding only nearest neighbors, in systems B and C two, and for systems D and E even more ''types'' of molecules exist. Consequently, for these systems the calculated spectra consist of a superposition of modes. For system B the peak positions are shifted to lower values compared to the random configurations, while for the systems C, D, and E the values are a bit higher. Apart from this, these systems are comparable with the random configurations, in the sense that the relaxation function does not decay exponentially for small t and the spectra are asymmetrical. As expected for these cases, since $\varphi(t)$ decays faster than system A but slower than the random systems, the values of the FWHM are high compared to system A but less than those of the random configu-

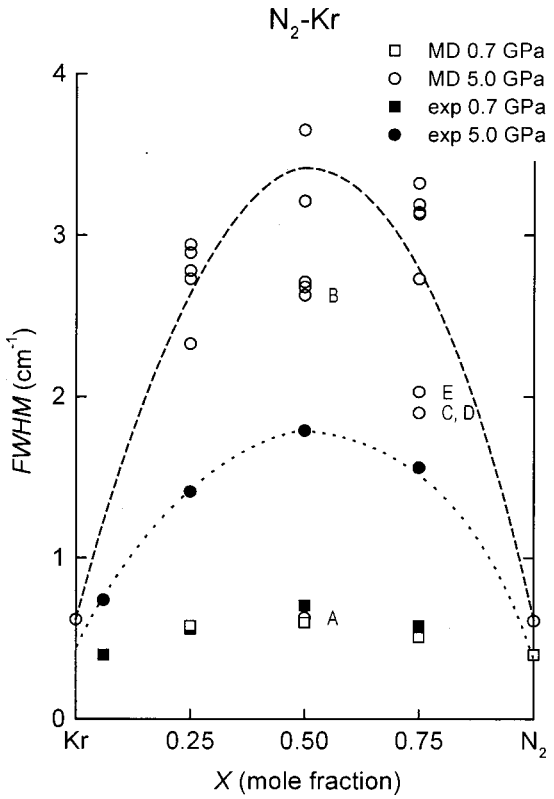

FIG. 7. FWHM vs the mole fraction for N_2 diluted in Kr at 0.7 GPa (squares) and 5.0 GPa (circles). Solid symbols: experimental data; open symbols: MD simulations. Squares: fluid phase; circles: homogeneous hcp phase. Dashed and dotted lines: guides to the eye through the simulation data with random configurations and through experimental points at 5 GPa. All experimental data points except those for pure N_2 have been obtained by linear interpolation. The experimental value of the frequency of pure β-N_2 at 5 GPa has been obtained by linear extrapolation, since nitrogen is in the δ phase at this pressure.

rations. The values for the amplitude of modulation and the frequency do not differ substantially from those of the random configurations. The spreading in Δ and in the relative frequency is about 3% for the distinct configurations.

Additionally, for the random configuration with $x=0.50$ at 5 GPa, four simulations have been performed during which the configuration is not ''static'' but instead, at equal time intervals, the positions, velocities, and rotations of two or more N_2 particles are interchanged while the frequency correlation function is not. Henceforth, this switching of quantities is referred to as ''swapping particles.'' If, for example, repeatedly 2 out of the 192 N_2 molecules swap in the time interval between two subsequent registrations (10^{-14} s), the average time needed for all molecules to swap once is about 1 ps. Hence, each N_2 particle remains for about 1 ps at a certain position and this value can be considered as the diffusion correlation time. By varying the number of molecules that simultaneously switch, the correlation time can be varied. In this way four simulations have been performed. The results are shown in Table II. It turns out that the obtained linewidths (second column) strongly depend on this diffusion correlation time.

Previous experimental results[25] showed a strong pressure dependence of the linewidth of N_2 in Kr in the solid phase

TABLE II. Calculated diffusion time and linewidth for the simulations with nonstatic configurations.

Diffusion time (ps)	FWHM (cm^{-1})
0.2	0.65
0.5	0.83
1	1.05
5	1.91
∞	3.04

while in neat β-nitrogen the linewidth barely increases with pressure. A possible cause for this different behavior could be that the diffusion slows down at increasing pressure. After all, in mixtures, slowing down of the diffusion results in line broadening. If this is the case, simulations with identical configurations should show a pressure dependence of the linewidth, similar to that of the pure system. To investigate this hypothesis, some subsequent simulations with identical static configurations have been performed for the 50 mol % mixture in the pressure range 0.7–9.75 GPa. In contrast to expectations, the results show a strong pressure dependence as can be seen in Fig. 8.

DISCUSSION AND CONCLUSION

It was found that the composition dependence of the frequency is mainly caused by the DC and not by the second order effect or the vibration-rotation coupling. Due to the high polarizability of krypton, at excitation of the nitrogen

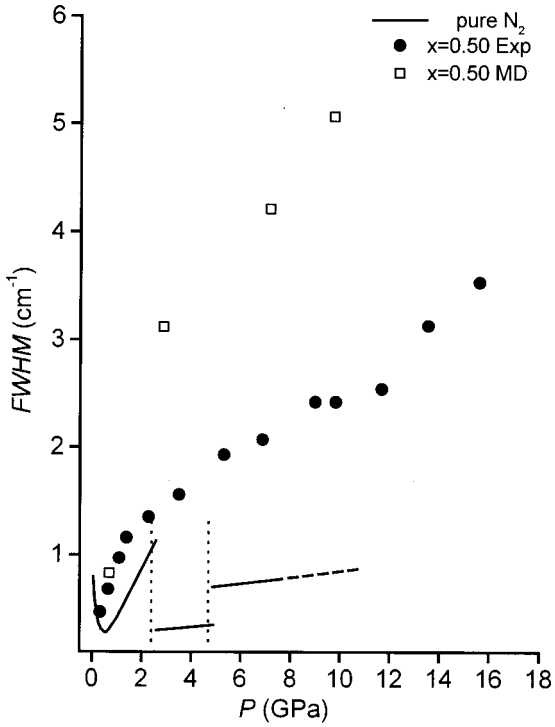

FIG. 8. Linewidth against pressure for the mixture with $x=0.50$. Squares: calculated widths with static, identical configuration; circles: experimental widths.

molecule, the DC for N_2 in N_2-Kr is relatively large (negative) compared to helium and neon in the systems previously investigated.

The amplitude of modulation as well as the vibrational frequency of nitrogen in krypton in the solid phase increase monotonically with x. For the frequency the dependence is linear. The latter effect has been reported for other binary systems with nitrogen in the fluid phase namely, N_2-He and N_2-Ne (Refs. 14 and 21, experimental and calculations) and N_2-Ar (Ref. 36, experimental). Because of the concentration dependence, all spectra originating from the mixtures, except for $x=0.50$, are asymmetrical. The asymmetry is reflected in the peak position of the spectra that deviate from the mean frequencies of the momentary distribution function, as can be seen from Table I comparing columns 5 and 6. Obviously, the asymmetry is caused by the fact that some frequencies occur more frequent than others. For example, in case C ($x=0.75$) the asymmetry is caused by the fact that 2/3 of all molecules is surrounded by 12 N_2 particles while 1/3 is surrounded by 9 N_2 and 3 Kr particles. In other words, more molecules with high frequencies (as in pure nitrogen) than molecules with lower frequencies exist. For the random systems, similar arguments are valid. For instance in the $x=0.75$ case the majority of the molecules will have 9 N_2 neighbors. Since there are more possibilities to have less than 9 N_2 neighbors than to have more, the spectrum shows a wing at the low-frequency side.

According to the Kubo theory,[23] for two limiting situations the line shape and width are given by simple expressions. In the fast modulation regime ($\Delta\tau_c \ll 1$) the line shape is Lorentzian and the linewidth can be calculated with

$$\mathrm{FWHM}=2\Delta^2\tau_c. \tag{11}$$

In the slow modulation regime ($\Delta\tau_c \gg 1$) the line shape reflects the momentary frequency distribution and the width is given by $\mathrm{FWHM}=2\Delta$.

In the solid, for the ''pure'' systems ($x=0$ and $x=1$) and system A, τ_c is equal to 0.0447, 0.0309, and 0.0363 ps, respectively. As mentioned before, these systems are clearly in fast modulation, as shown by the behavior of the relaxation function, the Lorentzian line shape and the small correlation time. With $\Delta\tau_c=0.054$, 0.042, and 0.047, respectively, the Kubo condition ($\Delta\tau_c \ll 1$) is indeed satisfied. Further, the calculated widths, using Eq. (11) (0.62, 0.61, and 0.63), are equal to those obtained from the relaxation function (Table I, column 3). Note that, although for the mixtures with random static configurations the line shape is nearly Gaussian and the FWHM is very large, these systems are still not in the slow modulation regime, since the widths are much (5–10 times) smaller than 2Δ. Apparently, the effect of motional narrowing is still rather strong.

Bondarev and Mardaeva[24] argue that the band broadening around $x=0.50$ in liquid mixtures is due to concentration inhomogeneities. In addition, Knapp and Fischer[1,5] and Moser *et al.*[6,11] assume the existence of several environments, caused by different numbers of neighboring particles. The authors reason that each environment produces a specific profile and the total spectrum shows, due to partly overlapping frequencies, one broad line. If this is the case, then the broadening effect at $x=0.50$ is caused by a maximum of the amplitude of modulation around $x=0.50$. However, as mentioned earlier, previous investigations have shown that Δ increases linearly with concentration. On the other hand, a strong increase in the correlation time was found around $x=0.50$ (Ref. 22). Therefore, it seems very plausible that, in liquid mixtures, in contrast to the arguments of Knapp and Fischer, the influence of diffusion is considerable, so that in a relatively short time each molecule encounters all possible surroundings. Müller *et al.*[37] reported Raman echo experiments on CH_3I in a 50 mol % liquid mixture with $CDCl_3$. They measured a finite lifetime for the concentration fluctuations (4–7 ps). In contradiction with conclusions of Knapp and Fischer, Müller *et al.* identified the source of the inhomogeneous broadening as concentration fluctuations in the time domain.

In the simulation model for the solid, the situation is quite different, since the configuration is static, apart from vibrations around the lattice positions, and different molecules see different but static surroundings. In this case, the calculated spectrum does reflect the concentration distribution and the line broadening is (partly) due to the number of possible surroundings. Clearly this effect is strongest for random distributions at equal mole fractions and the linewidth indeed shows a maximum at this value. In this case the amplitude of modulation is not a linear function of the concentration but is curved, due to the concentration effect.

In contrast with the liquid mixture (squares in Fig. 7), in the mixed solid (circles) the calculated linewidth is much larger compared to the experiment. There is an interesting way to explain the discrepancy. Since for the simulation data depicted in Fig. 7 the configuration is static, molecules with different surroundings vibrate around a different average value, resulting in an infinite correlation time. In fact, this looks like the case described in Refs. 4, 5, 10, and 11. In the real system, two possible situations could occur. In the first situation the particles do not swap or the time scale of the exchange is long compared to the time scale relevant for the modulation; thus, we have many different ''types'' of molecules and $P(\omega)$ consists of a superposition of many modes and therefore the spectrum consists of many peaks. Although the width of each individual peak can be reduced, the envelope can still be quite broad. If, on the other hand, the nitrogen and krypton particles rapidly switch places in the solid (as in the fluid), each molecule will vibrate with all possible frequencies and the momentary frequency distribution $P(\omega)$ consists of a single peak. The width of the modulated signal $I(\omega)$ is less than in the first case. The discrepancy between the calculated and experimental width can then be explained, assuming that in the real system, also in the solid phase, diffusion takes place at a time scale small enough to account for the modulation. Hence, via interpolation of the data given in Table II, a rough estimation of the diffusion correlation time can be made. The obtained value, that corresponds to a FWHM equal to the experimental value (1.8 cm^{-1}) is about 5 ps. Surprisingly, this life time is of the same order of magnitude as the values (4–7 ps) measured by Müller *et al.*[37] on a liquid 50 mol % mixture of CH_3I in $CDCl_3$.

A discrepancy is seen between the real system and the

simulation results where no diffusion occurs throughout the whole run (1000 ps). It is well known that, in small systems with a fixed volume, large local density fluctuations do not occur, although, on the other hand, the larger the system, the higher the chance that the local fluctuations are large enough to allow for particles to swap. Unfortunately, it is hard to determine minimum size of the system above which swaps may occur.

In contrast to expectations, the results of the simulations as function of pressure (Fig. 8) show a strong pressure effect on the linewidth. The dependence is even a bit stronger than in the real system. The strong increase of the linewidth with pressure in the real system can therefore not solely be attributed to a decrease of the diffusion rate at increasing pressure. On the other hand, experiments showed that the frequencies for the various concentrations diverge at increasing pressure. Hence, in the simulations, the individual peak positions of the various molecules with different surroundings diverge and the total spectrum becomes broader with pressure. In the real system this pressure effect is less strong due to the diffusion.

It should be mentioned that, next to diffusion, also resonance coupling could account for line narrowing. In fact, with his mechanism not the particles but the phonons interchange. However, with the applied procedure, we can not make a distinction between the two mechanisms.

The calculated frequencies for the various random configurations show a close resemblance to the experimental value and the spreading for each concentration is small. In the case of $x=0.75$, the clustered and layered configurations show significantly higher frequencies. Considering the small spreading, a deviation of 1.5 cm^{-1} is very large. Therefore, also the frequencies provide information about the configuration in the real system, and since the calculated frequencies for the random configurations show a closer resemblance to the experimental values than those of the systems B–E, it is suggested that, in real systems, the configuration is not clustered but random.

The fact that, for systems A and B, the frequencies are lower while for the systems C, D, and E these are higher than those of the random configurations can be explained by the following. For systems C, D, and E, the N_2 particles are clustered and most of them have only N_2 as nearest neighbors. Therefore, the frequencies are higher compared to the random configurations with $x=0.75$. In system B, for half of the molecules 4 out of 12 and for the other half 6 out of 12 neighbors are nitrogen molecules. Hence, the frequencies are lower than those of the random configuration with $x=0.50$. For system A obviously, since all N_2 particles have 6 N_2 neighbors, the frequencies are similar to those of the random systems with $x=0.50$.

In summary, comparison of the calculated frequencies with the experimental values points to random configurations in the mixed solids, while comparison of the calculated and experimental linewidth suggests a rapid exchange of the positions of the molecules.

[1] S. F. Fischer and A. Laubereau, Chem. Phys. Lett. **35**, 6 (1975).
[2] D. W. Oxtoby, Annu. Rev. Phys. Chem. **32**, 78 (1981).
[3] K. S. Schweizer and D. Chandler, J. Chem. Phys. **76**, 2296 (1982).
[4] E. W. Knapp and S. F. Fischer, J. Chem. Phys. **74**, 89 (1981).
[5] E. W. Knapp and S. F. Fischer, J. Chem. Phys. **76**, 4730 (1982).
[6] J. Chesnoy and G. M. Gale, Adv. Chem. Phys. **70**, 299 (1988).
[7] X. C. Zeng and D. W. Oxtoby, J. Chem. Phys. **93**, 4357 (1990).
[8] D. Ben-Amotz and D. R. Herschbach, J. Phys. Chem. **97**, 2295 (1993).
[9] G. S. Devendorf and D. Ben-Amotz, J. Phys. Chem. **97**, 2307 (1993).
[10] G. Moser, A. Asenbaum, and G. Döge, J. Chem. Phys. **99**, 9389 (1993).
[11] G. Moser, A. Asenbaum, J. Barton, and G. Döge, J. Chem. Phys. **102**, 1173 (1995).
[12] M. I. M. Scheerboom and J. A. Schouten, Phys. Rev. E **51**, R2747 (1995).
[13] G. S. Devendorf, D. Ben-Amotz, and L. E. S. de Souza, J. Chem. Phys. **104**, 3479 (1996).
[14] D. W. Oxtoby, D. Levesque, and J. J. Weis, J. Chem. Phys. **68**, 5528 (1978).
[15] D. Levesque, J. J. Weis, and D. W. Oxtoby, J. Chem. Phys. **72**, 2744 (1980).
[16] D. Levesque, J. J. Weis, and D. W. Oxtoby, J. Chem. Phys. **79**, 917 (1983).
[17] M. F. Herman and B. J. Berne, J. Chem. Phys. **78**, 4103 (1983).
[18] M. I. M. Scheerboom, J. P. J. Michels, and J. A. Schouten, J. Chem. Phys. **104**, 9388 (1996).
[19] J. P. J. Michels, M. E. Kooi, and J. A. Schouten, J. Chem. Phys. **108**, 2695 (1998).
[20] M. E. Kooi, J. P. J. Michels, and J. A. Schouten, J. Chem. Phys. **110**, 3023 (1998).
[21] N. Chayathri and B. Bagchi, J. Chem. Phys. **110**, 539 (1999).
[22] M. E. Kooi, J. P. J. Michels, and J. A. Schouten, J. Chem. Phys. **112**, 1404 (2000).
[23] R. Kubo, in *Fluctuation, Relaxation, and Resonance in Magnetic Systems*, edited by Ter Haar (Oliver and Boyd, Edinburgh, 1962), pp. 23–68.
[24] A. F. Bondarev and A. I. Mardaeva, Opt. Spektrosk. **35**, 286 (1973).
[25] H. T. Lotz and J. A. Schouten, Phys. Rev. B **64**, 184101 (2001).
[26] J. P. J. Michels, M. I. M. Scheerboom, and J. A. Schouten, J. Chem. Phys. **103**, 8338 (1995).
[27] J. P. J. Michels, M. I. M. Scheerboom, and J. A. Schouten, J. Chem. Phys. **105**, 9748 (1996).
[28] J. P. J. Michels and J. A. Schouten, Mol. Phys. **91**, 253 (1997).
[29] M. E. Kooi, F. Smit, J. P. J. Michels, and J. A. Schouten, J. Chem. Phys. **112**, 1395 (2000).
[30] R. D. Etters, V. Chandrasekharan, E. Uzan, and K. Kobashi, Phys. Rev. B **33**, 8615 (1986).
[31] E. A. Mason and W. E. Rice, J. Chem. Phys. **22**, 843 (1954).
[32] M. I. M. Scheerboom and J. A. Schouten, J. Chem. Phys. **105**, 2553 (1996).
[33] A. Mulder, J. P. J. Michels, and J. A. Schouten, J. Chem. Phys. **105**, 3235 (1996).
[34] J. P. J. Michels, M. E. Kooi, and J. A. Schouten, J. Chem. Phys. **108**, 2695 (1998).
[35] B. Lavorel, R. Chaux, R. Saint-Loup, and H. Berger, Opt. Commun. **62**, 25 (1987).
[36] H. T. Lotz and J. A. Schouten, Phys. Rev. B **64**, 024103 (2001).
[37] L. J. Müller, D. Vanden Bout, and M. Berg, J. Chem. Phys. **99**, 810 (1993).